Underpotential Deposition of Copper on Iodine-Modified Pt(111): In Situ STM and ex Situ LEED Studies

ARTICLE *in* THE JOURNAL OF PHYSICAL CHEMISTRY B · APRIL 1998

Impact Factor: 3.3 · DOI: 10.1021/jp9804143

6 AUTHORS, INCLUDING:

Junji Inukai
University of Yamanashi
100 PUBLICATIONS **1,725** CITATIONS
SEE PROFILE

Mitsuru Wakisaka
University of Yamanashi
31 PUBLICATIONS **736** CITATIONS
SEE PROFILE

Youn-Geun Kim
California Institute of Technology
85 PUBLICATIONS **786** CITATIONS
SEE PROFILE

Kingo Itaya
Tohoku University
246 PUBLICATIONS **8,355** CITATIONS
SEE PROFILE

Underpotential Deposition of Copper on Iodine-Modified Pt(111): In Situ STM and ex Situ LEED Studies

J. Inukai, Y. Osawa, M. Wakisaka, K. Sashikata, Y.-G. Kim,† and K. Itaya*

Department of Applied Chemistry, Graduate School of Engineering, Tohoku University, Aoba-yama 04, Sendai 980-8579, Japan

Received: December 4, 1997; In Final Form: February 9, 1998

The dynamic process of underpotential deposition (UPD) of copper on iodine-modified Pt(111) electrode in sulfuric acid solution was investigated by in situ scanning tunneling microscopy and ex situ low-energy electron diffraction. Prior to the copper deposition, iodine adlayer structures were characterized by both techniques. It was found that well-ordered iodine adlayers with the structures of (3×3) and $(\sqrt{7} \times \sqrt{7})$R19.1° could be prepared by immersion of the electrode in a solution containing iodide ions under potential control. It was also found that the interconversion of the two structures was very slow. After the UPD of copper on the iodine-modified Pt electrode, the iodine atoms formed a $c(p \times \sqrt{3}$R-30°) structure with a p value of ca. 2.6 on the (1×1) copper adlayer on Pt(111). After the copper was stripped, the electrode exhibited a mixture of (3×3) and $(\sqrt{7} \times \sqrt{7})$R19.1° structures of iodine on Pt(111).

Introduction

The underpotential deposition (UPD) of metal ions on single-crystal electrodes has long been investigated because it is important to understand how UPD processes are determined by the atomic structure of the surface.[1,2] It is well-known that UPD is strongly affected by the surface orientation of single-crystal electrodes as well as coadsorbed anions. The UPD of Cu on Au(111) in sulfuric acid is one of the most intensively investigated reactions by various techniques such as chronocoulometry,[3] scanning tunneling microscopy (STM),[4,5] atomic force microscopy (AFM),[6] low-energy electron diffraction (LEED) employing ultrahigh vacuum-electrochemical techniques (UHV-EC),[7] and X-ray techniques.[8] According to the recent X-ray scattering determination of the first adlayer of Cu on Au(111),[8] the Cu adatoms form a honeycomb lattice with a surface coverage of $^2/_3$, while a sulfate anion is coadsorbed at the center of each honeycomb unit cell forming a simple $(\sqrt{3} \times \sqrt{3})$R30° structure with respect to Au(111). Although in situ STM[4,5] and AFM[6] showed the image corresponding to the simple $(\sqrt{3} \times \sqrt{3})$R30°, the bright spots observed by these techniques should be considered as being due to adsorbed sulfate ions. On Pt(111), we have previously shown that in situ STM also yielded an image of the simple $(\sqrt{3} \times \sqrt{3})$R30° for the first UPD layer of Cu in sulfuric acid,[9] suggesting that the honeycomb lattice might also be formed on Pt(111). Although detailed studies have been carried out in order to evaluate the role of coadsorbed anions such as chloride,[10,11] it is more important to evaluate the role of sulfate/bisulfate anions in the UPD of Cu on Pt(111).

The Ag adlayers on iodine-modified Pt(111) and Au(111) electrodes have also been intensively investigated with surface structure-sensitive techniques such as ex situ LEED[2,12,13] and in situ STM.[14,15] Our STM study confirmed that the iodine adlayer structure was converted from $(\sqrt{7} \times \sqrt{7})$R19.1° to (3×3) by the formation of the first adlayer of Ag attached directly on the Pt surface,[13] which is in good agreement with the finding reported by Hubbard et al.[12,13] However, the STM images acquired after the second UPD could not explain the LEED patterns with three split spots reported previously.[13]

Hubbard and co-workers also carried out an ex situ LEED work on the UPD of Cu on I-modified Pt(111) (I−Pt(111)) in 1 M $NaClO_4$.[16] They observed a set of three spots near the position of a genuine $(\sqrt{3} \times \sqrt{3})$R30° and proposed a (10×10) structure.[16] On the other hand, it has been known that a similar LEED pattern appears on chlorine adlayers on Cu(111) surfaces in UHV, which has long been interpreted as a $(6\sqrt{3} \times 6\sqrt{3})$R30° structure.[17,18] Ito et al. carried out in situ STM of this system, reporting a $(\sqrt{3} \times \sqrt{3})$R30° structure.[19] These discrepancies strongly suggest that the structure of Cu on I−Pt(111) is more complicated than that found previously.[16−19]

It is important to note that all LEED patterns observed for iodine adlayers on Au(111) indicated rectangular adlattices which are assigned to $c(p \times \sqrt{3}$R-30°), the so-called $c(p \times \sqrt{3})$, where p is a variable parameter.[20,21] The decrease of p indicates compression of the rectangular adlattice only in one direction. When p is equal to 3, the structure is $(\sqrt{3} \times \sqrt{3})$R30°. Our interpretation for the iodine adlayer on Au(111) is consistent with the in situ X-ray scattering study carried out by Ocko et al.[22]

The aim of the present paper is to establish the adlayer structure after the UPD of Cu and to confirm the compression of the iodine layer on top of the Cu monolayer on Pt(111). We also describe the potential dependence of iodine adlayer structures on Pt(111) in the absence of Cu layers.

Experimental Section

In Situ Measurements. Pt single-crystal beads were prepared at the end of a Pt wire (99.99%) by the method described previously.[9,23] The well-prepared Pt bead consisted of (111) facets in an octahedral configuration. For voltammetric mea-

† Itaya Electrochemiscopy Project, ERATO/JST, 2-1-1 Yagiyama-minami, Taihaku-ku Sendai 982, Japan.

S1089-5639(98)00414-9 CCC: $15.00
Published on Web 04/11/1998

surements, the Pt(111) single crystal was mechanically polished with an accuracy of ca. 0.1°. The Pt(111) electrode was annealed in a hydrogen−oxygen flame for at least 2 h to remove surface damages caused by mechanical polishing. For STM experiments, one of the (111) facets was used. As the final pretreatment to expose clean Pt(111) surfaces, the single-crystal electrode was annealed in a hydrogen−oxygen flame and then quickly brought into contact with ultrapure water saturated with hydrogen. It is important to immerse the Pt(111) in the solution containing iodide ions under potential control in order to prepare a well-defined adlayer of iodine, as will be described in detail in the following section.

For the preparation of I-modified Pt electrodes (I−Pt), a clean Pt electrode was immersed into a 0.05 M H_2SO_4 + 1 mM KI solution at a specific potential for 5 min. The electrode was then rinsed in ultrapure water. The I−Pt(111) electrode was transferred to a 0.05 M H_2SO_4 + 1 mM $CuSO_4$ solution at 0.8 V for the study of Cu UPD.

Electrochemical measurements were carried out in a three-compartment glass cell with a reversible hydrogen electrode (RHE) as a reference electrode in 0.05 M H_2SO_4. Solutions were deoxygenated by bubbling with purified N_2.

In situ STM measurements were carried out with a Nanoscope E (Digital Instruments). The STM tips used were made of electrochemically etched Pt−Ir (80:20) wires. To minimize residual background currents, the side wall of the tips was coated with nail polish.

Ex Situ LEED. LEED and AES experiments were performed in an ultrahigh vacuum (UHV) system that consisted of analysis, preparation, and electrochemical (EC) chambers as described previously.[20] The analysis chamber was equipped with retarding-field optics for LEED and AES (Omicron Vacuumphysik GmbH, Germany). A commercial Pt(111) single-crystal disk electrode (MaTecK, Material-Technologie & Kristalle GmbH, Germany) was initially cleaned by multiple cycles of thermal annealing and Ar^+-ion bombardment, followed by final annealing at 1000 K for 10 min to restore atomic smoothness. Iodine adsorption was carried out by immersion of the UHV-prepared electrode in the EC chamber under potential control. The EC chamber was backfilled with ultrapure Ar prepared by using a high-temperature Ti-getter chamber.[20] Two different solutions of 0.05 M H_2SO_4 + 0.1 mM KI and 0.01 M $KClO_4$ + 0.1 mM KI adjusted to pH 4 with HI were used for the preparation of iodine adlayers on Pt(111). The latter solution was identical to that employed for the previous LEED study.[24] The same solution, 0.05 M H_2SO_4 + 1 mM $CuSO_4$, was used for the LEED study of the UPD of Cu.

All solutions were prepared with H_2SO_4 (Cica-Merck, ultrapur grade), KI (Kanto Chemical, Cica reagent grade), $CuSO_4$ (Merck, proanalysi grade), $HClO_4$ (Cica-Merck, Ultrapur grade), HI (Kanto Chemical, Cica reagent grade), and ultrapure water (Millipore-Q).

Results and Discussion

Voltammetric Study. Hubbard and co-workers have intensively investigated the structure of the iodine adlayer on Pt(111) in aqueous iodide solution using the UHV-EC technique.[2,24] They conclusively demonstrated that the adlayer structures, mainly the commensurate (3 × 3) and ($\sqrt{7}$ × $\sqrt{7}$)R19.1°, were formed on the well-defined Pt(111)−(1 × 1) surface, depending on the electrode potential and pH of the solution. For example, in a solution containing 10 mM $KClO_4$ and 0.1 mM KI, adjusted to pH 4 with HI, they found the (3 × 3) and ($\sqrt{7}$ × $\sqrt{7}$)R19.1° structures in anodic and cathodic potential ranges, respectively (see Figure 4 in ref 24). Although previous STM studies revealed various atomic structures of iodine on Pt in air and in solution,[25−28] no direct in situ STM evidence of the potential dependence was reported. It has long been expected, at least by us, that the transformation between the two structures should take place reversibly when the electrode potential was changed in the double-layer region.

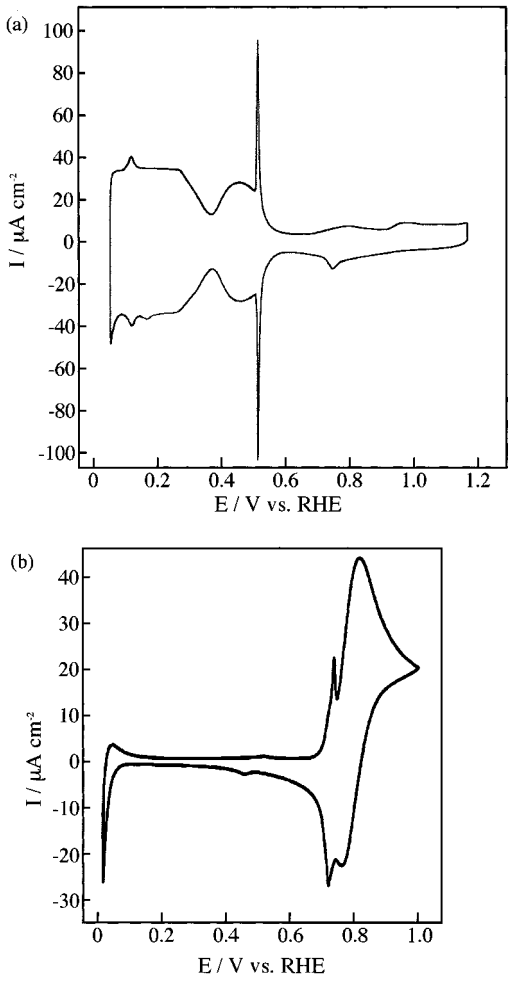

Figure 1. (a) Cyclic voltammogram for Pt(111) electrode in 0.05 M H_2SO_4; scan rate, 50 mV s^{-1}. (b) Cyclic voltammogram for Pt(111) electrode in 0.05 M H_2SO_4 + 1 mM KI; scan rate, 5 mV s^{-1}.

Our recent article described that the structural transformation did occur upon changing the electrode potential but it was extremely slow.[30] Two structures of (3 × 3) and ($\sqrt{7}$ × $\sqrt{7}$)R19.1° usually coexisted even after the electrode potential was changed in the double-layer region. Besides the above result, it was found in this study that the immersion potential is the most important factor in determining the iodine adlayer structure.

We first briefly describe cyclic voltammetry (CV) of Pt(111) in a sulfuric acid solution in the absence and presence of KI and then discuss in situ STM and ex situ LEED experiments. Figure 1a and b shows typical CV's for a well-defined Pt(111) in 0.05 M H_2SO_4 in the absence of KI and in a solution of 0.05 M H_2SO_4 + 1 mM KI, respectively. The highly reversible characteristic peaks observed on Pt(111) in pure H_2SO_4 disappeared in the solution containing KI, leaving a featureless double-layer region between 0.1 and 0.65 V. A voltammetric study was also carried out in the same solution (0.01 M $KClO_4$ + 0.1 mM KI, adjusted to pH 4 with HI) as was used for the previous work. The result was identical to that reported

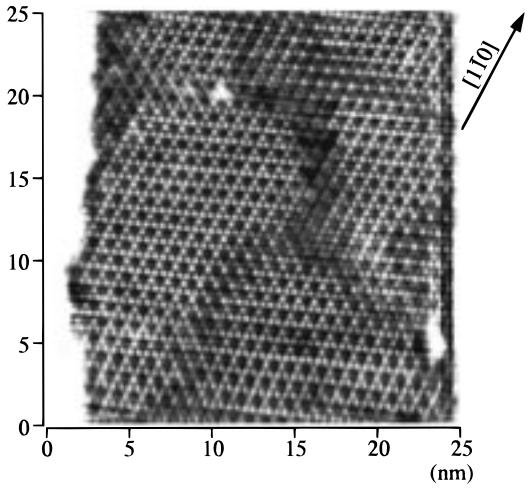

Figure 2. In situ STM image for (3 × 3) structure of I−Pt(111) surface in 0.05 M H_2SO_4 + 1 mM KI; scanning range, 25 × 25 nm^2; electrode potential for immersion and STM observation, 0.6 V.

previously.[24] In the presence of KI, the characteristic peaks of a clean Pt(111) for the hydrogen adsorption−desorption reaction were completely eliminated by the adsorption of iodide ions. The cathodic current observed at potentials near 0 V is mainly due to the hydrogen evolution reaction rather than the desorption of iodine adlayer. In the anodic region, the broad anodic peak at ca. 0.8 V is mainly due to the oxidation of iodide ions in solution because the peak height is proportional to the square root of scan rate and to the concentration of iodide ions. Note that a pair of sharp peaks at ca. 0.72 V is proportional to the scan rate, suggesting that a surface redox reaction might take place prior to the oxidation of iodide ions in solution.

When the electrode was transferred into pure H_2SO_4 after the CV shown in Figure 1b was recorded, a featureless voltammogram extended over the range of 1 V with small capacitance values of 10−15 μC/cm^2. The oxidation current commencing at ca. 1.1 V steeply increased at more anodic potentials, which is attributed to oxidation of adsorbed iodine. Similar oxidation peaks were observed on an I−Au(111) as described previously.[15]

In Situ STM and ex Situ LEED. A highly ordered (3 × 3) adlayer was found to form when the flame-annealed Pt(111) was immersed at 0.6 V in the solution used for Figure 1b. The open circuit potential was measured to be 0.66 V in the same solution. Figure 2 shows a typical high-resolution STM image acquired in a relatively large area at the potential of 0.6 V. The entire area including that near the step edges was completely covered with iodine atoms with relatively large domains of a (3 × 3) structure. It was previously shown by STM that there are two different (3 × 3) structures, namely asymmetric and hexagonal (symmetric) lattices.[27] Although the asymmetric lattice is predominant in Figure 2, well-ordered symmetric domains were also observed on the same terrace. These two different adlattices were found with an almost equal probability. These results are consistent with those reported previously.[27]

On the other hand, Figure 3 shows typical examples of STM images acquired when the clean Pt(111) was immersed in the iodide-containing H_2SO_4 solution at 0.15 V. Even in the large area of 100 × 100 nm^2, Figure 3a, the atomically flat terraces were predominantly covered with iodine adlattices possessing a ($\sqrt{7}$ × $\sqrt{7}$)R19.1° structure, which can be seen more clearly in Figure 3b. The (3 × 3) structure as marked by the solid lines was found occasionally on the surface. Although the above results are in good agreement with those of Hubbard,

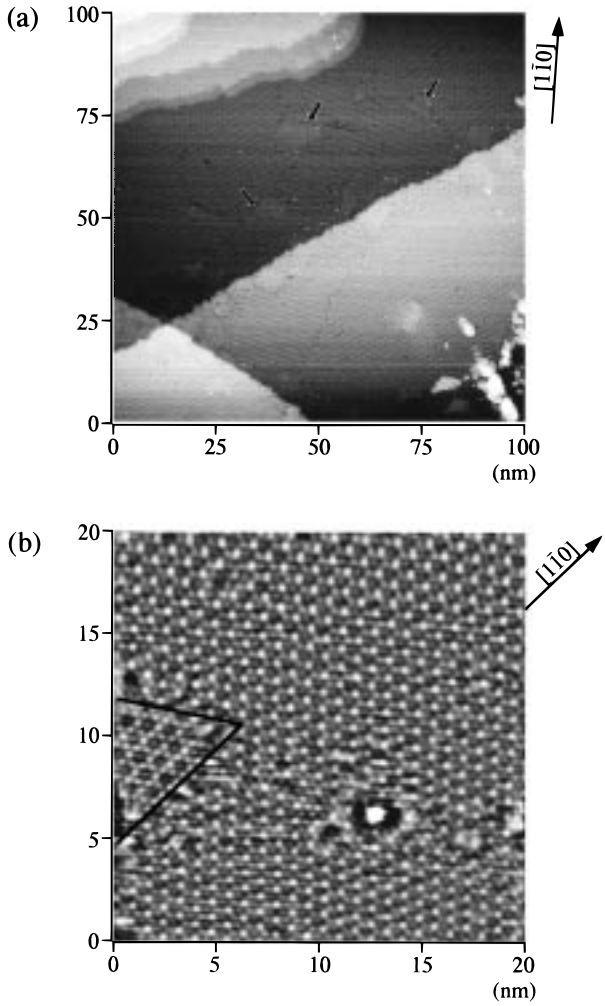

Figure 3. In situ STM images of I−Pt(111) surface mainly showing ($\sqrt{7}$ × $\sqrt{7}$)R19.1° structure of iodine in 0.05 M H_2SO_4 + 1 mM KI. Electrode potential for immersion and STM observation = 0.15 V. (a) Scan range, 100 × 100 nm^2; small domains with (3 × 3) structure are indicated by arrows. (b) Scan range, 20 × 20 nm^2; a small (3 × 3) domain is seen on the left.

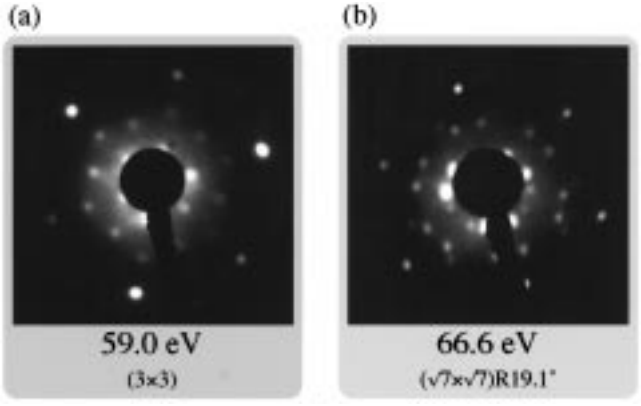

Figure 4. LEED patterns for I−Pt(111). (a) Electrode potential for immersion and emersion, 0.6 V; incident beam energy, 59.0 eV. (b) Electrode potential for immersion and emersion, 0.15 V; incident beam energy, 66.6 eV.

no interconversion between the ($\sqrt{7}$ × $\sqrt{7}$) and (3 × 3) adlattice structures was found to take place when the electrode potential was changed within the double-layer region.

Figure 4a and b shows LEED patterns obtained for the electrode immersed in and then emersed from the same iodide-

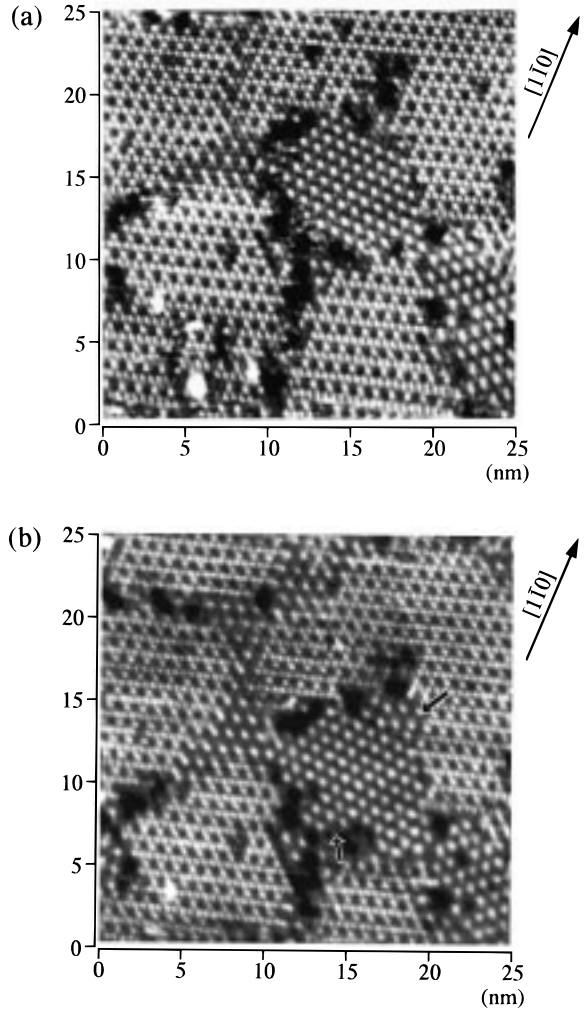

Figure 5. Potential-dependent change in the adlayer structure of iodine on Pt(111) in 0.05 M H_2SO_4 + 1 mM KI. Scanning range, 25 × 25 nm^2. (a) Electrode was immersed and observed by in situ STM at 0.45 V. (b) 10 min after the potential was stepped from 0.45 to 0.15 V. Small domains of (3 × 3) are seen to be incorporated in ($\sqrt{7} \times \sqrt{7}$)R19.1° structures as indicated by the arrows.

containing H_2SO_4 solution at potentials of 0.6 and 0.15 V, respectively. These LEED patterns correspond to the (3 × 3) and ($\sqrt{7} \times \sqrt{7}$)R19.1° structures, respectively, indicating that the surface was covered with each well-defined adlayer.

On the contrary, in situ STM clearly showed both of the structures to coexist on the Pt(111) surface when the clean Pt(111) electrode was immersed into the solution at a potential between 0.3 and 0.5 V. A typical example is shown in Figure 5a, which was obtained at an immersion potential of 0.45 V. A ($\sqrt{7} \times \sqrt{7}$) domain can be clearly seen at the center of the image, surrounded by the (3 × 3) domains. The potential-dependent structural change was directly probed by a time-dependent in situ STM experiment. When the electrode potential was stepped from 0.45 to 0.15 V after the acquisition of the image shown in Figure 5a, the second image shown in Figure 5b was obtained after 10 min, indicating that the interconversion between the two structures was very slow. Only a few iodine atoms marked by arrows were incorporated into the ($\sqrt{7} \times \sqrt{7}$) domain. This result provides direct evidence that the surface diffusion of iodine atoms is very slow on Pt(111).

A different set of experiments was carried out in 0.05 M H_2SO_4 in the absence of iodide ions. A well-defined

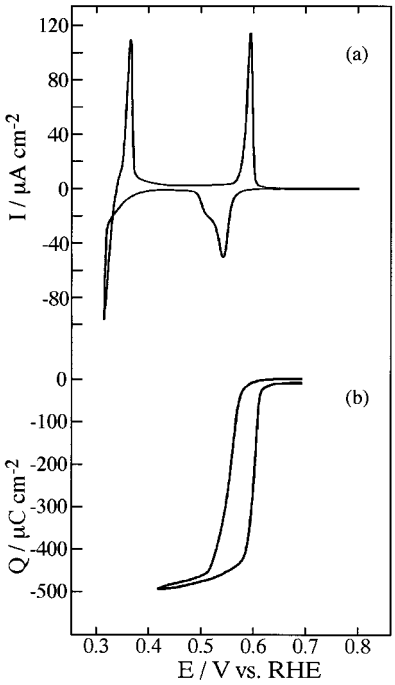

Figure 6. (a) CV and (b) CC for I−Pt(111) electrode in 0.05 M H_2SO_4 + 1 mM $CuSO_4$; scan rate, 5 mV s^{-1}.

I−Pt(111) electrode with the (3 × 3) structure prepared at 0.6 V as described above structure was immersed into 0.05 M H_2SO_4. Then, STM images were recorded at various electrode potentials. It was found that the (3 × 3) structure was consistently observed at least for 30 min even when the electrode potential was held at 0.15 V. A similar experiment was also done for I−Pt(111) with the ($\sqrt{7} \times \sqrt{7}$) adlattice. The ($\sqrt{7} \times \sqrt{7}$) structure persisted for a long time even at 0.6 V. These results suggest that the iodine atoms are attached on Pt(111) through a chemical bond. The initially formed structure was practically invariable by changing the electrode potential. Although it is still unclear why the two ordered structures appear at the different potentials, the formation of chemical bonds between iodine and Pt atoms is likely to be affected by the electrode potential. In the ($\sqrt{7} \times \sqrt{7}$)R19.1° structure, iodine atoms should be located on either atop or 3-fold hollow sites. In the hexagonal (3 × 3) structure, iodine atoms are expected to be located on bridge and atop sites. The asymmetric atop and 3-fold hollow sites are the expected positions for the asymmetric (3 × 3) structure.[27] We strongly feel that a theoretical calculation is needed to explain the effect of potential on the adlayer structure.

UPD of Cu on I−Pt(111). Figure 6 shows CV (a) and cyclic coulometric (CC) (b) curves for I−Pt(111) in 0.05 M H_2SO_4 + 1 mM $CuSO_4$. The iodine adlayer was prepared at 0.6 V in the solution containing KI. The CV is very different from that for bare Pt(111) obtained in the same solution,[9] indicating a large influence of the surface iodine on the UPD of Cu. The UPD of Cu appears as a cathodic peak at 0.54 V associated with a shoulder. The cathodic current commencing at 0.35 V is due to the bulk deposition of Cu. The corresponding anodic peak at 0.38 V is due to the desolution of the deposited bulk Cu. The anodic sharp peak at 0.6 V corresponds to the desorption of the UPD layer. The overall shape of the UPD of Cu is very similar to that reported previously.[16] The deposition of more than 10 layers of bulk Cu did not alter the shape of the UPD peaks in CV, indicating that the well-defined surface of I−Pt(111) was not damaged by the bulk deposition. It is also

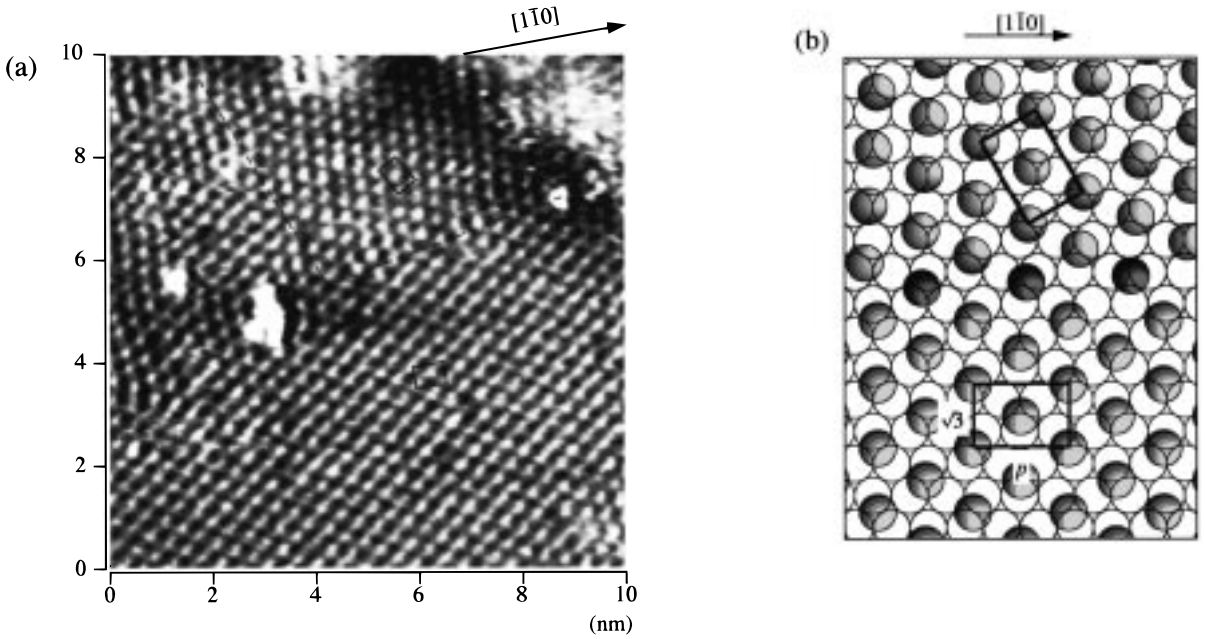

Figure 7. (a) In situ STM image of I−Pt(111) in 0.05 M H_2SO_4 + 1 mM $CuSO_4$ after UPD of Cu; electrode potential, 0.48 V. (b) Structural model: open circle, Cu; shaded circle, iodine.

noteworthy that an almost identical CV was observed for the I−Pt(111) with the $(\sqrt{7} \times \sqrt{7})$ structure, suggesting that the UPD of Cu is not a structure-sensitive reaction with respect to the initial structures of iodine on Pt(111).

The CC curves show that the same amount of charge was consumed for the adsorption and desorption of UPD Cu, and it was calculated to be ca. 480 μC cm^{-2} between 0.7 and 0.4 V. We previously reported almost the same value for the UPD of Cu on bare Pt(111) in the sulfuric acid solution.[9] If Cu^{2+} ions were totally discharged to Cu^0 during the UPD reaction, the measured charge corresponds to the coverage of 1.0 for Cu. Although a smaller value of 0.84 was reported previously,[12] we believe that a full monolayer formed after the UPD peak. A full monolayer of Cu is known to form on Au(111) after the second UPD peak.[3]

In situ STM observations were carried out to determine the structure of the adlayer after the UPD of Cu. An I−Pt(111) with the (3×3) iodine adlayer was first immersed in 0.05 M H_2SO_4 + 1 mM $CuSO_4$ at 0.7 V. In the potential range between 0.8 and 0.58 V before the UPD, the (3×3) structure of iodine was consistently observed as described above. To determine the adlayer structure after the UPD as accurately as possible, it was necessary to minimize distortion in STM images frequently caused by thermal drift. Before the UPD, we waited until an almost ideal hexagonal symmetry was observed for the iodine adlayer on Pt(111). It was clearly demonstrated in our previous investigations that high-resolution STM measurements performed with minimal thermal drift in $x-y$ directions make it possible to discriminate between closely related structures such as $(\sqrt{3} \times \sqrt{3})$R30°, $c(p \times \sqrt{3})$,[20,21] and $(5 \times \sqrt{3})$.[15]

Under such carefully adjusted experimental conditions, a typical high-resolution STM image was obtained as shown in Figure 7a, which was acquired at 0.45 V. It was consistently found that there was significant distortion of atomic rows from the 3-fold symmetry expected for the $(\sqrt{3} \times \sqrt{3})$R30° structure. The image shown in Figure 7a cannot be interpreted as the $(\sqrt{3} \times \sqrt{3})$R30° adlayer. More importantly, the image shows domain boundaries as indicated by the dashed lines. The atomic rows are rotated by 60° at the boundary. A centered rectangular unit cell is superimposed in each domain in Figure 7a. Such rotational domain does not exist for the $(\sqrt{3} \times \sqrt{3})$R30° adlayer. The length of the shorter sides of each unit cell corresponds to $\sqrt{3}$ times the Pt−Pt distance, and they are tilted by 30° from the atomic rows of the Pt(111) substrate ([1$\bar{1}$0]). The length of the longer sides corresponds to ca. 2.5−2.6 times the Pt−Pt distance. Besides determining the lattice parameters of the iodine adlayer, it is also important to note that all iodine atoms in the STM image show the same corrugation height. There is no sign of height difference among the iodine atoms. Such a flat feature of the STM image suggests that all iodine atoms on top of the Cu layer are located on similar sites. These findings are basically the same as those reported previously for the iodine adlayers on Au(111) and Ag(111).[20,21,31,32] We proposed a model structure, $c(p \times \sqrt{3}$R-30°), to explain the in situ STM images and LEED patterns. Figure 7b shows an atomic arrangement near the phase boundary. All iodine adatoms are located on the "unit cell bisectors", defined as the planes which are vertical to the substrate and include 2-fold bridge sites.[20] The p value evaluated from the STM image is equal to 2.5−2.6.

Thus, it can be concluded that an incommensurate structure of iodine exists on the (1×1) commensurate structure of Cu on Pt(111). Note that the p value continuously changed from 3 to 2.5 in the case of the iodine adlayer on Au(111).[20,21] Although we expected that the p value might vary in the potential range between 0.4 and 0.48 V, the STM images acquired in this potential range were identical and resulted in the same p value.

We also investigated the iodine structure after complete desorption of Cu. Figure 8 shows a typical STM image obtained at 0.8 V after the desorption of Cu. It is of interest to note that the (3×3) iodine structure initially observed as shown in Figure 2 is now converted partially to the $(\sqrt{7} \times \sqrt{7})$R19.1° structure. Both the (3×3) and $(\sqrt{7} \times \sqrt{7})$R19.1° structures consistently coexisted after the desorption of the Cu layer. About 50% of the surface showed the $(\sqrt{7} \times \sqrt{7})$R19.1° structure. A similar experiment was also carried out using an I−Pt(111) with $(\sqrt{7} \times \sqrt{7})$R19.1°. At potentials more anodic than the

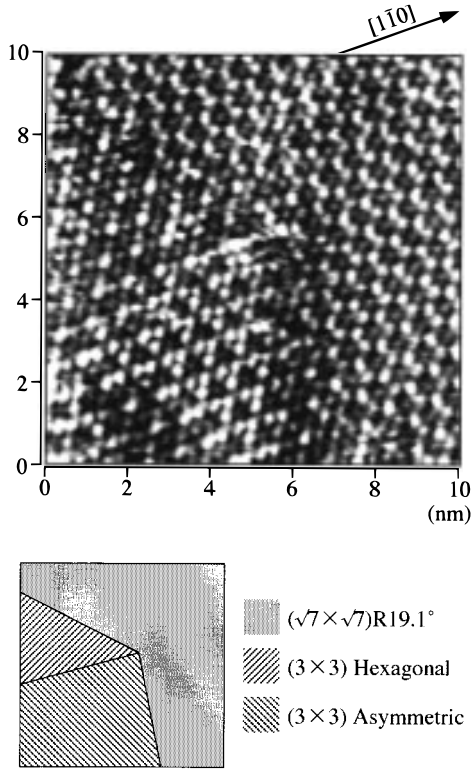

Figure 8. In situ STM image of I−Pt(111) in 0.05 M H_2SO_4 + 1 mM $CuSO_4$, after desorption of Cu; electrode potential, 0.8 V. Both (3 × 3) and ($\sqrt{7} \times \sqrt{7}$)R19.1° structures are seen to coexist.

potential for UPD, the ($\sqrt{7} \times \sqrt{7}$)R19.1° structure was predominantly observed in 0.05 M H_2SO_4 + 1 mM $CuSO_4$, whereas an image almost identical to that shown in Figure 7 was obtained after the UPD, indicating strongly that the structure of the topmost layer of iodine is independent of the initial iodine structure on Pt(111). Moreover, a coexisting structure similar to that shown in Figure 8 was observed after the desorption of the Cu layer. In view of the fact that the two structures, (3 × 3) and ($\sqrt{7} \times \sqrt{7}$)R19.1°, are not easily converted to each other in pure sulfuric acid solutions, it can be stated that the UPD of Cu created a new reaction path for the structural conversion of adsorbed iodine. Since the two structures coexist, they must be similarly stable, while the potential barrier may be large for the structural transformation.

Ex Situ LEED. It was demonstrated in our previous papers that complementary use of in situ STM and ex situ LEED is a powerful technique for characterizing iodine adlayers on various substrates such as Au, Ag, and Pd.[33,34] For detailed analyses, LEED and AES measurements were carried out using a UHV-EC apparatus. Figure 9 shows a set of LEED patterns for the UPD of Cu on an I−Pt(111) with the (3 × 3) structure. A clear (3 × 3) pattern was observed by LEED before the UPD was initiated as shown in Figure 9a. After completion of the UPD of Cu, LEED patterns showed split spots near the $\sqrt{3}$ position and spots for a (1 × 1) structure as shown in Figure 9b. These (1 × 1) spots were found at the same position as was observed before the UPD, indicating that the Cu layer has the commensurate (1 × 1) structure on Pt(111). A closer inspection of the LEED pattern obtained at 26.8 eV, Figure 9c, reveals that the inner spots are triply split. The LEED pattern with three split spots should be assigned to $c(p \times \sqrt{3}\text{-R30°})$ as described above. Using the analytical method for the LEED pattern described in our previous papers,[20,21] we calculated the p value as 2.6 ± 0.05 from the LEED pattern shown in Figure

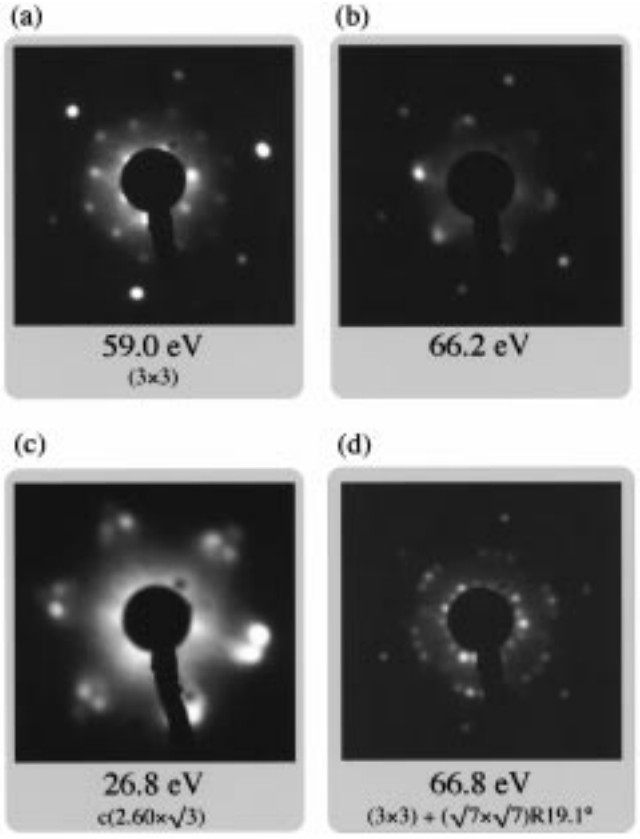

Figure 9. LEED patterns for I− Pt(111). (a) Emersion from 0.05 M H_2SO_4 + 1 mM KI at the open circuit potential (before UPD); incident beam energy, 59.0 eV. (b) Emersion from 0.05 M H_2SO_4 + 1 mM $CuSO_4$ at 0.48 V (after UPD); incident beam energy, 66.2 eV. (c) Emersion from 0.05 M H_2SO_4 + 1 mM $CuSO_4$ at 0.48 V (after UPD); incident beam energy, 26.8 eV. (d) Emersion from 0.05 M H_2SO_4 + 1 mM $CuSO_4$ at 0.8 V (after Cu desorption); incident beam energy, 66.8 eV.

9c, which is in good agreement with the value obtained from the in situ STM shown in Figure 7. Note that the nearest neighbor distance in the iodine adlayer becomes almost equal to that of the van der Waals' diameter of iodine atom (0.43 nm) when $p = 2.6$, suggesting that the most compressed structure in the incommensurate $c(p \times \sqrt{3})$ appeared after the UPD of Cu. The same LEED pattern was obtained on I−Pt-(111) with the ($\sqrt{7} \times \sqrt{7}$)R19.1° structure.

After the desorption of the UPD Cu at 0.8 V, the LEED pattern shown in Figure 9d was obtained. It can be interpreted as a simple sum of the spots corresponding to the (3 × 3) and ($\sqrt{7} \times \sqrt{7}$)R19.1° structures. This is in agreement with the STM results showing the two coexisting domains. The spot intensities for both patterns were similar, indicating that neither of the two structures is dominant on the surface. Stickney et al. reported that the ($\sqrt{7} \times \sqrt{7}$)R19.1° structure reappeared after the desorption of the Cu layer in 1 M $NaClO_4$.[12] Although the discrepancy between their results and ours is difficult to explain, it is noteworthy that a similar LEED pattern indicating the coexistence was found in the present acidic solution. The effect of pH might be an important factor influencing the structure of the iodine adlayer on Pt(111) after the desorption of the Cu layer.

Our AES data agreed with those previously reported by Stickney et al.[12] Before the UPD of Cu, AES peaks for iodine were clearly observed. The UPD of Cu yielded an AES peak for Cu, but it disappeared on the desorption of Cu. The intensity

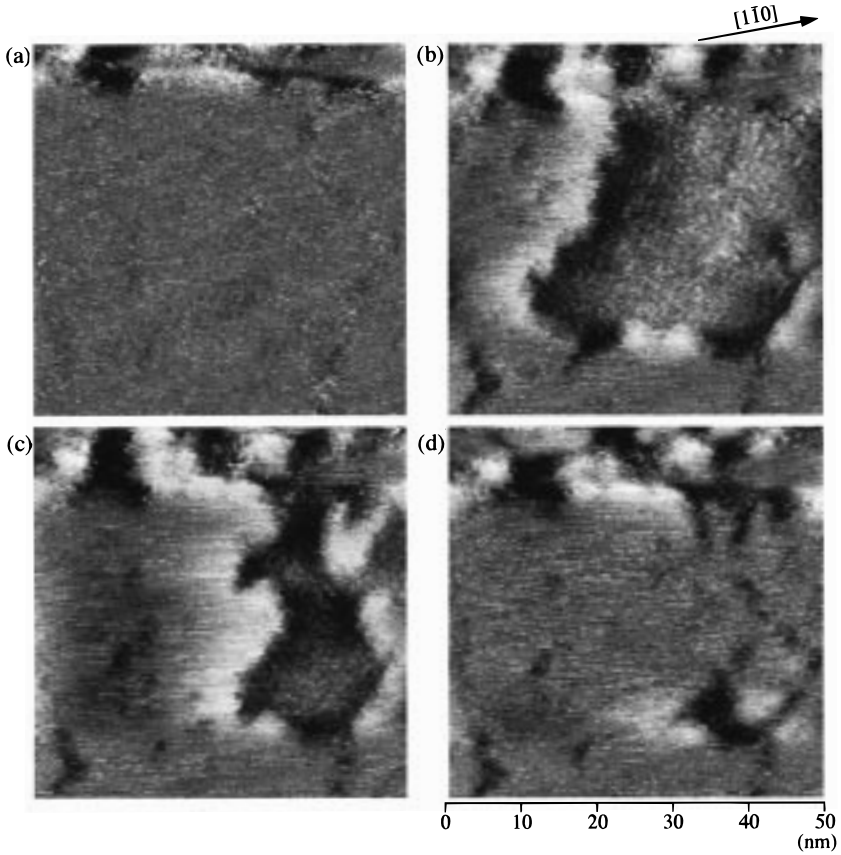

Figure 10. Time-sequenced STM images of I−Pt(111) during the UPD of Cu: (a) before the start, (b) after 20 s, (c) after 50 s, (d) after 80 s of UPD at 0.48 V in 0.05 M H_2SO_4 + 1 mM $CuSO_4$. Each image was obtained in 12 s.

of iodine peak did not change before and after the UPD, indicating that the iodine atoms existed on the topmost surface layer as described previously.[12]

Finally, we also investigated the iodine adlayer structure after the bulk deposition of Cu on I−Pt(111) and also on a bulk Cu(111) single-crystal electrode. Our ex situ LEED and in situ STM indicated the formation of the simple ($\sqrt{3} \times \sqrt{3}$)R30° structure on the Cu(111) surface, which is consistent with the result of a LEED analysis reported previously.[35] The difference between the $c(p \times \sqrt{3}$-R30°) structure on Cu/Pt(111) and the ($\sqrt{3} \times \sqrt{3}$)R30° structure on Cu(111) can be explained in terms of different Cu−Cu distances in the two kinds of copper. The first Cu layer forms the (1 × 1) structure on Pt(111) as described above, indicating that the nearest distance of Cu atoms is the same as that of Pt(111), or 0.278 nm, while that on the bulk Cu(111)−(1 × 1) is 0.256 nm. The distance between nearest iodine atoms in the ($\sqrt{3} \times \sqrt{3}$)R30° structure on Cu(111) is calculated to be 0.44 nm, which is very close to the van der Waals' diameter of iodine atom of 0.43 nm.[20,22] Thus, the ($\sqrt{3} \times \sqrt{3}$)R30° structure of iodine layer on Cu(111) nearly corresponds to the close-packed structure.

Dynamic Processes of UPD. Time-dependent STM imaging reveals dynamic processes of UPD. Figure 10 shows a series of STM images acquired during the UPD of Cu in an area of atomically flat terrace. After acquiring the image (a) at 0.6 V, the electrode potential was stepped to 0.47 V, where the formation of a Cu layer should be completed at an equilibrium condition according to the CV shown in Figure 6. After 20 s of the potential step, the atomically flat terrace was gradually covered with a Cu adlayer. The initial stage of the UPD was found to be the formation of small islands, which occurred randomly on the I−Pt(111) terrace. Such islands grew laterally. The step lines seen in the image (b) had a height of 0.2 nm, which is equal to the height of the Cu layer. Therefore, the newly formed terraces are thought to have resulted from the UPD of Cu. The lower terrace is expected to be the Cu free area where the iodine is attached on Pt(111). The higher terrace continuously grew as shown in Figure 10c, and the surface of I−Pt(111) was almost completely covered with the Cu layer after 80 s as shown in Figure 10d. The gradual growth of the islands seemed to occur without a long-range preferential growth along the atomic rows of either substrate or adsorbed iodine. However, jagged features of the step lines might suggest a short-ranged preferential growth of the island.

Figure 11 shows a high-resolution STM image obtained at 0.56 V near the UPD peak of Cu. The (3 × 3) structure of iodine is observed on the lower terrace in the right half of Figure 11, and the $c(p \times \sqrt{3})$ structure on the newly formed upper terrace. The unit cells of the (3 × 3) and $c(p \times \sqrt{3}$R-30°) structures are shown on the lower and upper terraces, respectively. The close-packed direction of Pt(111) substrate, [1$\bar{1}$0], is indicated by the arrow in Figure 11. The longer side of the rectangular unit cell is parallel to the [1$\bar{1}$0] direction, while the shorter side is rotated by 30° with respect to the close-packed direction. The result shown in Figure 11 indicates that the $c(p \times \sqrt{3}$R-30°) structure appeared at an initial stage of the UPD. We did not find the (3 × 3) structure which was previously reported to form during the UPD.[12]

Acknowledgment. This work was partially supported by a Grant-in-Aid for Scientific Research on Priority Area of "Electrochemistry of Ordered Interfaces" (No. 09237101) from the Ministry of Education, Science, Sports and Culture, Japan, and ERATO−Itaya Electrochemiscopy Project, JST. The authors

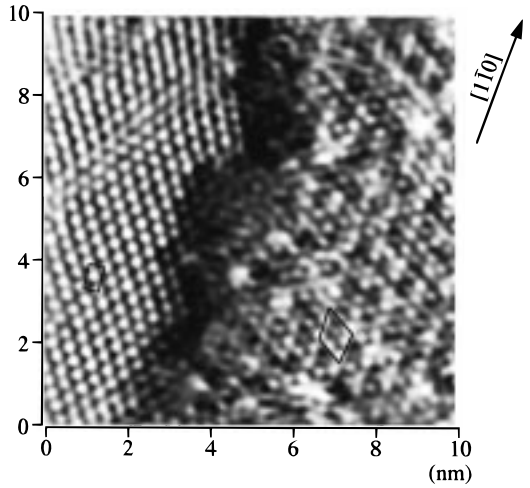

Figure 11. In situ STM image of I−Pt(111) in 0.05 M H_2SO_4 + 1 mM $CuSO_4$; electrode potential, 0.57 V. (Left) $c(p \times \sqrt{3}\text{R-}30°)$ structure of I on the UPD layer of Cu; (right) (3×3) structure of I on Pt(111).

thank Dr. Y. Okinana for his help in the writing of this manuscript, S. Tanaka in the LEED measurements, and M. Sugimasa in the STM observations.

References and Notes

(1) Kolb, D. M. In *Advances in Electrochemistry and Electrochemical Engineering*; Gerischer, H., Tobias, Ch. W., Eds.; Wiley: New York, 1978; Vol. 11, p 125.
(2) Hubbard, A. T. *Chem. Rev.* **1988**, *88*, 633.
(3) Shi, Z.; Lipkowski, J. *J. Electroanal. Chem.* **1994**, *365*, 303.
(4) Magnussen, O. M.; Hotlos, J.; Beitel, G.; Kolb, D. M.; Behm, R. J. *J. Vac. Sci. Technol.* **1991**, *B9*, 969.
(5) Hachiya, T.; Honbo, H.; Itaya, K. *J. Electroanal. Chem*. **1991**, *315*, 275.
(6) Manne, S.; Hansma, P. K.; Massie, J.; Elings, V. B.; Gewirth, A. A. *Science* **1991**, *251*, 183.
(7) Kolb, D. M. *Ber. Bunsen-Ges. Phys. Chem.* **1988**, *92*, 1175.
(8) Toney, M. F.; Howard, J. N.; Richer, J.; Borges, G. L.; Gorden, J. G.; Melroy, O. R. *Phys. Rev. Lett.* **1995**, *75*, 4472.
(9) Sashikata, K.; Furuya, N.; Itaya, K. *J. Electroanal. Chem*. **1991**, *316*, 361.
(10) Marković, N. M.; Gasteiger, H. Á.; Lucas, C. A.; Tidswell I. M.; Ross, P. N. *Surf. Sci.* **1995**, *335*, 91.
(11) Gomez, R.; Tee, G. M.; Feliu, J. M.; Abruña, H. D. *Surf. Sci*. **1995**, *335*, 101.
(12) Stickney, J. L.; Rosasco, S. D.; Song, D.; Soriaga, M. P.; Hubbard, A. T. *Surf. Sci.* **1983**, *130*, 326.
(13) Hubbard, A. T.; Stickney, J. L.; Rosasco, S. T.; Soriaga, M. P.; Song, D. *J. Electroanal. Chem*. **1983**, *150*, 165.
(14) Shinotsuka, N.; Sashikata, K.; Itaya, K. *Surf. Sci*. **1995**, *335*, 75.
(15) Sugita, S.; Abe, T.; Itaya, K. *J. Phys. Chem*. **1993**, *97*, 8780.
(16) Stickney, J. L.; Rosasco, S. D.; Hubbard, A. T. *J. Electrochem. Soc*. **1984**, *131*, 260.
(17) Doddard, P. J.; Lambert, R. M. *Surf. Sci*. **1977**, *67*, 180.
(18) Walter, W. K.; Manolopoulos, D. E.; Jones, R. G. *Surf. Sci*. **1996**, *348*, 115.
(19) Matsumoto, H.; Oda, I.; Inukai, J.; Ito, M. *J. Electroanal. Chem*. **1993**, *356*, 275.
(20) Yamada, T.; Batina N.; Itaya, K. *J. Phys. Chem*. **1995**, *99*, 8817.
(21) Batina, N.; Yamada, T.; Itaya, K. *Langmuir* **1995**, *11*, 1(11), 4568.
(22) Ocko, B. M.; Watson, G. M.; Wang, J. *J. Phys. Chem*. **1994**, *98*, 897.
(23) Yau, S.-L.; Kim, Y.-G.; Itaya, K. *J. Am. Chem. Soc*. **1996**,*118*, 7795.
(24) Lu, F.; Salaita, G. N.; Baltruschat, H.; Hubbard, A. T. *J. Electroanal. Chem*. **1987**, *222*, 305.
(25) Schardt, B. C.; Yau S.-L.; Rinaldi, F. *Science* **1989**, *243*, 1050.
(26) Yau, S.-L.; Vitus, C. M.; Schardt, B. C. *J. Am. Chem. Soc*. **1990**, *112*, 3677.
(27) Chang, S.-C.; Yau, S.-L.; Schardt, B. C.; Weaver, M. J. *J. Phys. Chem*. **1991**, *95*, 4787.
(28) Vogel, R.; Kamphausen, I.; Baltruschat, H. *Ber. Bunsen-Ges. Phys. Chem.* **1992**, *96*, 525.
(29) Shinotsuka, N.; Sashikata, K.; Itaya, K. *Surf. Sci*. **1995**, *335*, 75.
(30) Itaya, K. In *In Situ Local Probe Techniques for Studies of Electrochemical Interfaces*; Lorenz, W. J., Plieth, W., Eds.; IUPAC Monograph, in press.
(31) Yamada, T.; Ogaki, K.; Okubo, S.; Itaya, K. *Surf. Sci*. **1996**, *369*, 321.
(32) Yamada, T.; Batina, N.; Ogaki, K.; Okubo, S.; Itaya, K. In *Electrode Processes VI: Proceedings of the Sixth International Symposium*; Wieckowski, A., Itaya, K., Eds.; The Electrochemical Society: Pennington, 1996.
(33) Soriaga, M. P.; Schimpf, J. A.; Carrasquillo, A., Jr.; Abreu, J. B.; Temesghen, W.; Barriga, R. J.; Jeng, J.-J.; Sashikata, K.; Itaya, K. *Surf. Sci.* **1995**, *335*, 273.
(34) Schimpf, J. A.; Abreu, J. B.; Soriaga, M. P.; Sashikata, K.; Itaya, K. In *Electrode Processes VI: Proceedings of the Sixth International Symposium*; Wieckowski, A., Itaya, K., Eds.; The Electrochemical Society: Pennington, 1996.
(35) Dicenzo, S. B.; Wertheim, G. K.; Buchanan, D. N. E. *Surf. Sci.* **1982**, *121*, 411.